Basrah Journal for Engineering Sciences, Vol. 20, No. 2, (2020), 60-65

Basrah Journal for Engineering Sciences

Journal homepage: www.bjes.edu.iq
ISSN (Online): 23118385, ISSN (Print): 18146120

OPEN ACCESS

Measurement and Prediction of Residual Stresses in Low Carbon Steel Pipes Welded Shielded Metal Arc Welding

Salah Sabbar Miftin [1,*], Haidar Maath Mohammed [2], Ameen Ahmed Nassar [3]

[1,3]*Department of Mechanical Engineering, College of Engineering, University of Basrah, Basrah, Iraq*
[2]*Department of Material Engineering, College of Engineering, University of Basrah, Basrah, Iraq*
E-mail address: salahsabbar82@gmail.com , drhaidermaath@gmail.com, aaledani@gmail.com
Received: 8 January 2020; Accepted: 11 February 2020; Published: 2 March 2020

Abstract

Welding is carried out with a very complex thermal cycle, which results in irreversible elastic-plastic deformation, and residual stresses in and around fusion zone and heat-affected zone (HAZ). A residual stress due to welding arises from the differential heating of the pipes due to the weld heat source. However, due to the presence of residual stresses in and around the weld zone the strength and life of the component is also reduced. The objective of this work is to measure the welding residual stress in ASTM (A-106 Gr. b) steel pipes with 4" diameter and 6 mm thickness welded manually (SMAW) in three-pass butt joint where shielded metal arc welding process consists of heating, melting and solidification of parent metals and a filler material in localized fusion zone by a transient heat source to form a joint between the parent metals. The welding process will have accrued without preheating and heat treatment. This measuring of residual stress occurs by using hole-drilling strain gauge method according to (ASTM E-873) then the experimental results for residual stresses obtained from welded carbon steel pipes used to provide validation for finite element simulations. The welding process and welding residual stress distribution is calculated by Ansys Finite Element techniques. Theoretical considerations can be assessed by a mechanical model. The overall, there is good agreement between the predicated and measured distributions of residual stress, but the magnitude of predicted stress tend to greater in welding region.

Keywords: Ansys, carbon steel pipe, finite element method, residual stresses, SMAW.

1. Introduction

Industrial pipes are very important for fluid transportation in the chemical, petrochemical, and petroleum industries. To assure the integrity of weld joints, the correct weld parameters / procedures must be selected to prevent the formation of defects, as well as to eliminate possible defects introduced by the welding. Some kinds of failure do not depend on preexisting defects and the vectors associated to the failure are generally difficult to be detected and it is not always possible to eliminate them, such as residual stresses [1]. Residual stresses arising from welding influence crack initiation, crack growth, and fracture processes. In general, the residual stresses are harmful and reduced component life, whereas compressive stresses are beneficial. For an accurate integrity assessment of welded carbon steel pipes, it is important to have a detailed knowledge of internal residual stresses and how they change during service. Such integrity assessment forms an input to decisions relating to safe operation of plant, life extension, and repair or replacement strategies [2].

Residual stresses are the stresses that exit within a component when there is no external load is applied to it. So, any remaining stress that exists in a process component either in thermal or mechanical method without any applied external loads can be identified as residual stress. In welding residual stresses arise due to the expansion and contraction of the weld metal and heat affected zone during local heating and subsequent cooling. There is no doubt that residual welding stresses can contribute fatigue and stress-corrosion cracking in specific environments in which such failure represents a hazard [1, 3].

The experimental work including preparing of different specimens of welded pipeline metals (ASTM A-106 Grade B) [4] then measuring of residual stress occurs by using hole-drilling strain gauge method according to (ASTM E-873) [5] then the experimental results for residual stresses obtained from welded carbon steel pipes used to provide validation for finite element simulations. The theoretical work involves a new approach to overcome the difficulties is to build and solve two models, the first model takes the thermal analysis and the second model deals with the mechanical analysis and then couple between them to simulate the interactions at different models by using computer software (ANSYS). The aim of this study was to develop FEM modal capable of predicting thermal history and residual stresses of carbon steel pipe weld with higher accuracy.

2. Simulation of Residual Stresses in Welded Carbon Steel Pipe

The welding process is essentially a coupled thermo-mechanical process. However, since the residual stress field is strongly dependent on the temperature field. Welding residual stress distribution is calculated by Ansys finite element technique. The method consists of two parts: a thermal analysis followed by a mechanical analysis. The following subsections explain the different analysis used for the present study.

2.1. Thermal Analysis

During welding the governing partial differential equation for the three-dimension transient heat conduction with internal heat generation is given by the thermal equilibrium equation [6]:

$$\frac{\partial}{\partial x}\left(K_x\frac{\partial T}{\partial x}\right)+\frac{\partial}{\partial y}\left(K_y\frac{\partial T}{\partial y}\right)+\frac{\partial}{\partial z}\left(K_z\frac{\partial T}{\partial z}\right)+Q=\rho c\frac{\partial T}{\partial t} \quad (1)$$

Where: T is the temperature (°C), K is the thermal conductivity (W/m.°C), c is the specific heat (J/kg.°C), ρ is the density (kg/m^3), t is the time (min), Q is the rate of heat generation per unit volume (W/m^3).

The heat flux is applied over the weld bead as the heat input to the thermal analysis [7, 8].

$$Q_1=\frac{\eta * I * V}{A} \quad (2)$$

$$q=\frac{\eta * I * V}{S} \quad (3)$$

Where: Q_1 is the supplied heat flux (W/mm^2) from the welding arc on the surface of the work piece at any distance, q is the arc power (J/mm), I is the welding current (Amp), V is arc voltage (Volt), S is the arc speed (mm/sec), A is the weld bead area (mm), and η is thermal efficiency for SMAW welding (75-80) [8].

This simulation program predicts the residual stress distribution of weldment material in accordance with the amount of metal volume change induced by the temperature variation in the welding process. Factors such as heat input, travelling speed of the weld filler metal, the thickness of the weld pipe, the geometry, and the temperature of the interpass [9]. The general solution to the differential equation governing heat conduction in a solid body is obtained by accepting the initial and boundary condition.

1. Initial conditions

At t = 0, $T_{\text{weld metal}}$ = 1530 °C, $T_{\text{workpiece}}$ = 30 °C, T_{air} = 30 °C.

2. Boundary conditions, the specific heat flow acting over surface will be that of surface convection and radiation according to:

$$K_n\frac{\partial T}{\partial n}=h\left(T_w-T_f\right)+\varepsilon\sigma\left(T_w^4-T_f^4\right) \quad (4)$$

Where: h is the heat transfer coefficient at the model surface; T_w is the temperature of the model surface; T_f is the temperature of the surrounding, ε is the radiation coefficient of the black body, and σ is the Stefan-Boltzmann constant.

2.2. Mechanical Analysis

The second step of the current analysis involves the use of the temperature histories computed by the pervious thermal analysis for each time increment as an input (thermal loading) for a thermal stress analysis. During welding process, as the melting temperature increases, the stress-strain increases, and the material enters a plastic state. The elastic strain increment is calculated using the isotropic Hooke's law with temperature-dependent Young's modulus and Poisson's ratio. The thermal strain increment is computed using the coefficient of thermal expansion. For the plastic strain increment, a rate-independent elastic-plastic constitutive equation is considered with the Von Mises yield criterion, temperature-dependent mechanical properties and linear isotropic hardening rule is used to calculate the elastic-plastic stress:

$$[d\sigma]=[D^{ep}]d\epsilon_{ij}-[C^{th}]dT \quad (5)$$

$$d\epsilon_{ij}=d\epsilon_{ij}^{e}+d\epsilon_{ij}^{p}+d\epsilon_{ij}^{th} \quad (6)$$

$$[D^{ep}]=[D^{e}]+[D^{p}] \quad (7)$$

Where: $d\epsilon_{ij}^{e}$ is the elastic strain increment, $d\epsilon_{ij}^{p}$ is the plastic strain increment, $d\epsilon_{ij}^{th}$ is the thermal strain increment, $[D^e]$ is the elastic stiffness matrix, $[D^p]$ is plastic stiffness matrix, $[C^{th}]$ is thermal stiffness matrix, and dT is the temperature increment [10].

2.3. Material Properties

Since welding processes undergo a high temperature cycle and exhibit material properties that are temperature dependent. It is a general statement in literature that special attention must be paid to the description of the material properties and its behavior if further advances in numerical modeling of welding phenomena have to be achieved. But it is also evident that the model and relevant properties need only represent the real material behavior with sufficient accuracy [11].

In the applications Ansys in the present work, both thermal and mechanical material properties of weld metal and heat affected zone are assumed to be the same as that of the base metal due to the lack of information on material properties of weld metal and heat affected zone, the material considered in this work is carbon steel pipe. The material properties are briefly in Figs. 1, 2, 3, 4, 5.

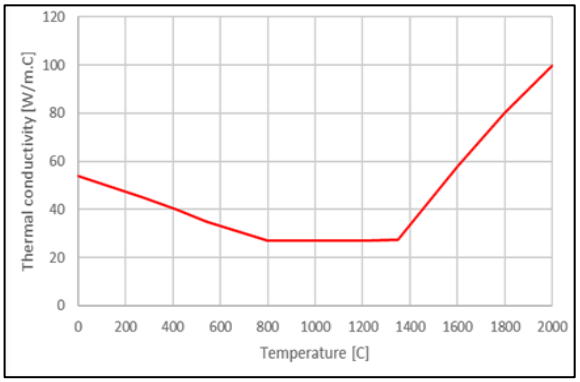

Fig 1 Thermal conductivity as function of temperature [11].

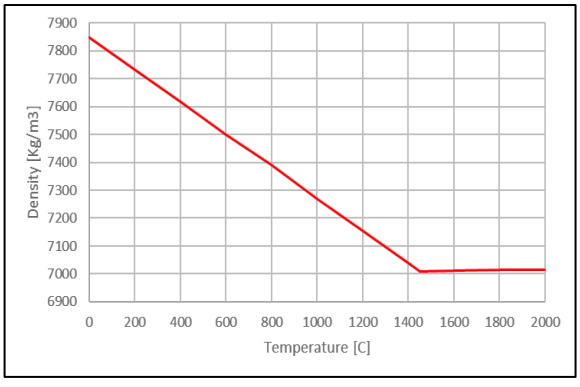

Fig 2 Density as function of temperature [12].

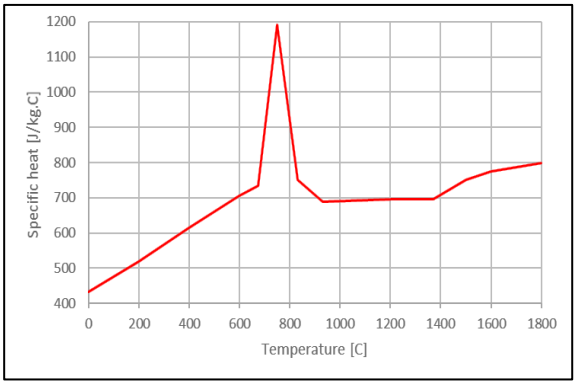

Fig 3 Specific heat as function of temperature [12].

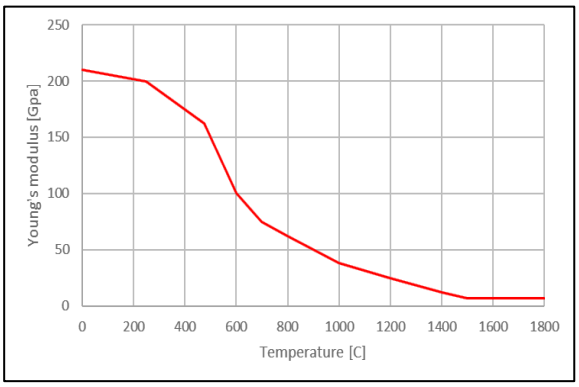

Fig 4 Young's modulus as function of temperature [11].

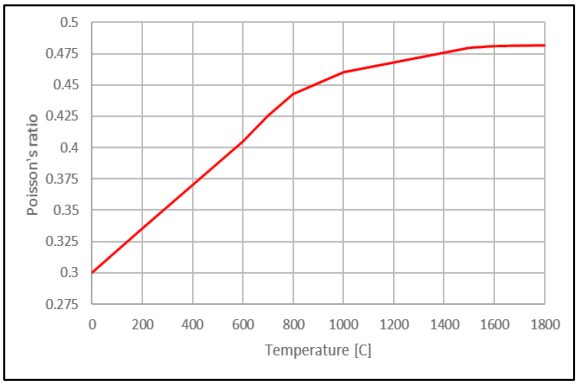

Fig 5 Poisson's ratio as function of temperature [11].

2.4. Numerical Simulation

The SMAW welding process is simulated through the Finite Element method using the Ansys software. The geometry and dimension of the pipe butt weld, which is made of carbon steel pipe (ASTM A106 Gr-b) [3] with outer diameter of 114.3 mm, thickness of 6 mm, and length 250 mm are schematically shown in Fig. 6. The pipe is welded by three passes where the welding arc travel direction and weld star/stop position (Θ = 0°) using the welding parameters shown in Table 1. Finite Element method of welding in Ansys program is carried out in two stages as transient thermal analysis and static structural analysis.

The boundary conditions were considered to transfer the convection and radiation heat. In the simulated model, 13974 linear cubic eight-node elements were used. The number of used elements were determined based on the analyzing the sensitivity of the elements. Therefore, the maximum number of displacing the pipe during a welding process was studied. Figure 7 shows that when the number of elements is equal to 13974, the maximum number of nodes is equal 64071.

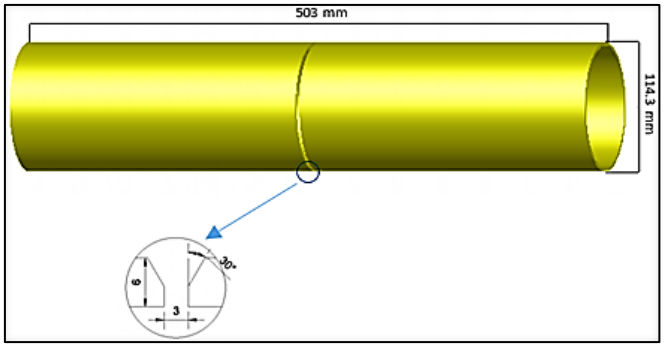

Fig 6 Dimension of analysis model.

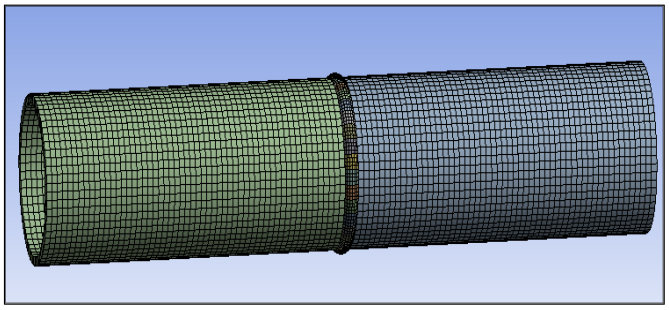

Fig 7 The elements used in analysis the FEM.

Table 1 The welding parameters of carbon steel pipe.

Number of passes	Amperage (A)	Voltage (V)	Speed (mm/sec)
3	80-110	23-25	5-8

3. Experimental Procedure

The carbon steel pipes were circumferential welded by using shielded metal arc welding method. In this method, two pipes with an outer diameter of 114.3 mm were used. The pipes were welded without preheating in three passes [ASME b31.1]. Experimental work was performed to calculate welding residual stresses and evaluate results of numerical analysis where a hole drilling strain gauge method was used according to ASTM E873 [ASTM]. A strain gauge rosette with three elements of the general type schematically illustrated in Fig. 9 is placed in the area under consideration and its specifications are shown in Table 2. The residual stresses in the area surrounding the drilled hole relax. The relieved strains are measured with a suitable strain-recording instrument; the resulting outputs of strains are designated e_1, e_2, and e_3.

Compute the stresses σ_{max} and σ_{min} from compute the following combination strains for each set of measured strains e_1, e_2, e_3:

$$p = (e_3 + e_1)/2 \tag{8}$$

$$q = (e_3 - e_1)/2 \tag{9}$$

$$t = (e_3 + e_1 - 2e_2)/2 \tag{10}$$

$$\sigma_{max}, \sigma_{min} = -E\left[\frac{p}{a(1+v)} \pm \frac{\sqrt{q^2 + t^2}}{b}\right] \tag{11}$$

Where: a and b are rosette strain gauge coefficients [5].

The following main weaknesses can be emphasized. First of all, the hole drilling strain gauge method is semi-destructive; hence a certain distance must be kept between adjacent measuring points not to affect each other. Secondly, only stresses at the surface of the material can be measured and finally the method must be carried out manually.

Table 2 Rosette Strain Gauge Specifications.

Type	OHMS	Gage Factor	Grade
BX120-1CG (1×1)	120 ± 0.2	2.08 ± 1 %	B

Fig 8 The sample before experimental test.

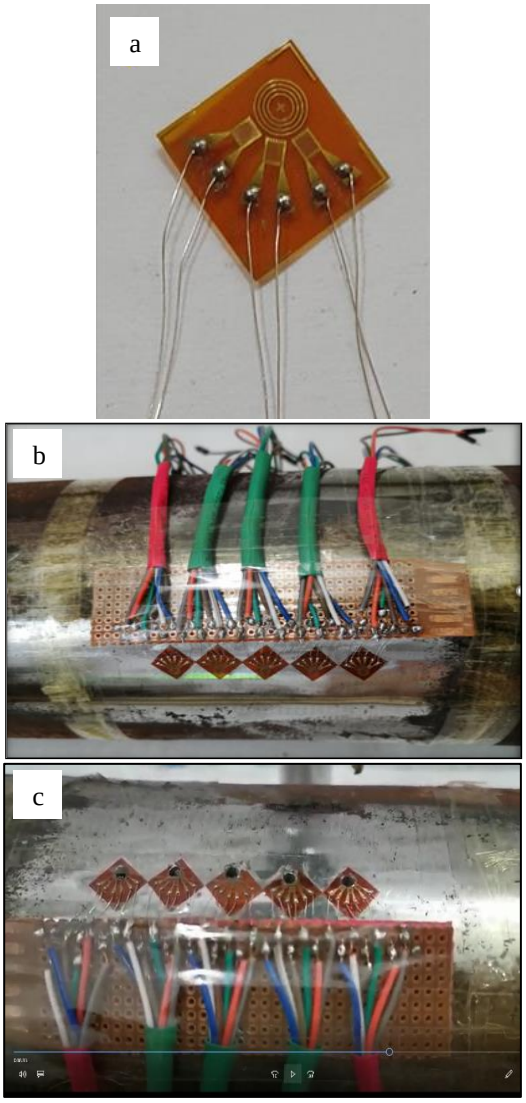

Fig 9 (a) Rosette strain gauge, (b) Before drilling pipe, (c) After drilling pipe.

4. Results and Discussion

The fundamental goal of this study was to develop a reliable FEM modal capable of predicting thermal history and residual stresses of carbon steel pipe weld with higher accuracy. The measurement residual stress by the hole drilling method is (611.78 MPa) at the welding center (zero mm) and its magnitude close to the prediction residual stress by Ansys program where the Fig. 10 shows results obtained FEM developed from welding centerline to the pipe edge. High residual stress occur in the welding center then increases in regions near the weld due to a resistance contraction of the material as cooling commences after that decreasing until reaches lower magnitude.

In general, the numerical results at the neighborhood of the center of the weld zone, the residual stress distribution forms a stable with a value of (628.56 MPa) approximately and increasing. Furthermore, the residual stress across the interface between weld zone and heat affected zone increases to maximum value about (747.59 MPa). On the other hand, in the heat affected zone of the weld the magnitude of the residual stress decreases sharply and reaches a minimum value at location of (50 mm) with a value close to zero, and this description for the residual stress on the carbon steel pipe sample, it is seen high similarity on the side centerline welding.

Although both the numerical and experimental results are considered to be in reasonably good agreement, small discrepancies can be observed. The difference between the calculated and measured results may be related to the discrepancy in the assumptions and simplifications of analysis, such as theoretical basis, temperature distribution and original residual stress, as well as inherent uncertainties of measurement, such as strain gauge placement, mechanical grinding and oxidation layer. The theory of the hole-drilling strain-gauge method is based on linear elastic mechanics. Therefore, the error in the measured residual stress will be enhanced as the value of the residual stress approaches the yield stress. Additionally, in the weld code the temperature distribution is approximated by a piecewise linear temperature change. This approach will give somewhat different results compared with the temperature actually experienced.

Because of the non-smooth surface caused by metal deposited during welding, the strain gauge placement on the welded specimen will influence the residual stress measurement if care is not taken. Moreover, the residual stress at the internal surface is obtained from the pipe surface, but that at the external surface is obtained directly from the weld pass. However, the good repeatability of experimental results shows that the effect of strain gauge placement is seen to be a minimum.

From the above discussion, it can be seen that the computational method not only conforms to the actual distribution of residual stress, but also shows good agreement with the results obtained by the experimental method. The results obtained from this study can be recognized as representative engineering data and can be further applied in field service.

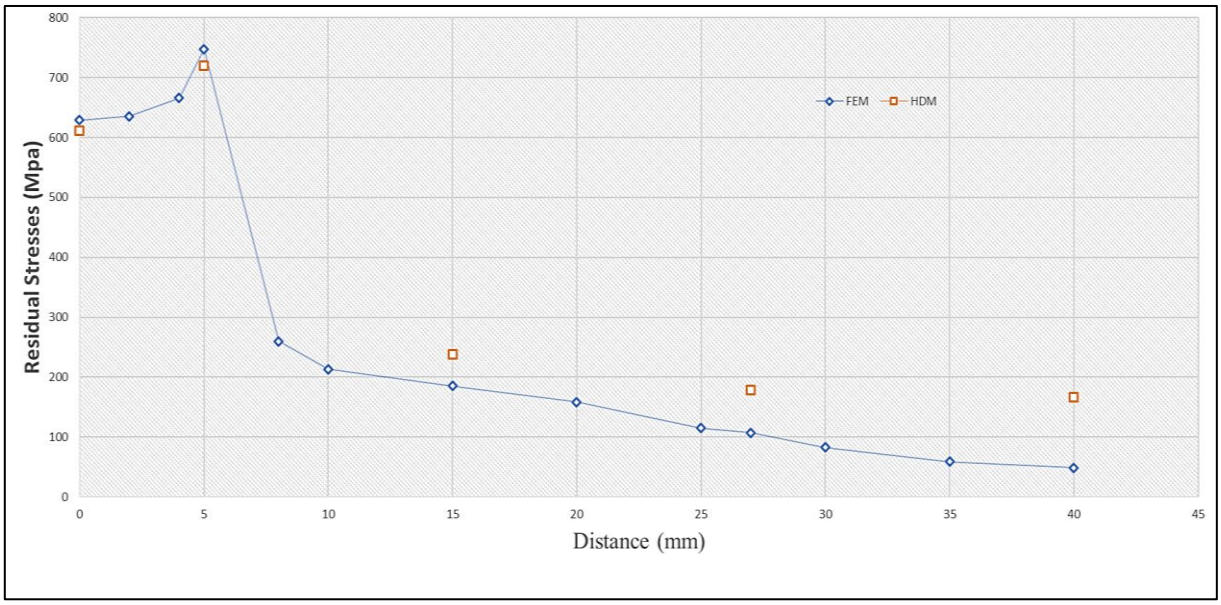

Fig. 10 Residual stresses from the welding centerline.

4.1. The Effect of the Voltage Change on the Residual Stress

The residual stress fields for welding voltage equal to 15, 19, 23, 27, and 30 Volt, which are used in the simulations, as shown in Fig. 11. The voltage of the welding is increased and therefor the heat input energy, which is a function of welding voltage, is increased. Then, it can be concluded that the level of induced residual stresses is increased.

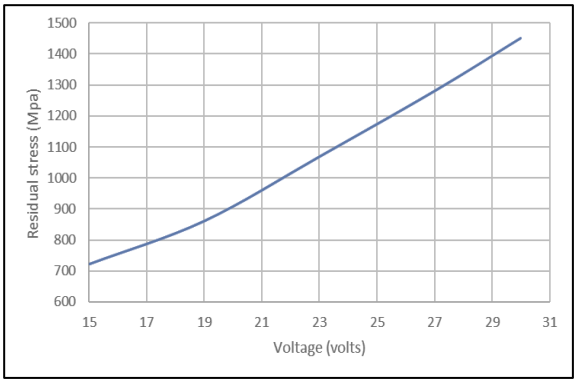

Fig 11 The Effect of the Voltage Change on the Residual Stress.

4.2. The Effect of the Amperage Changes on the Residual Stress

Figure 12 shows the residual stress in the outer surface of pipe for five different currents of 80, 86, 92, 101, and 110 Amp, holding all other variables constant. Increasing of the amperage causes the overall input heat increase. The effects of input heat is directly on the temperature distribution and the resulting residual stress graph in welded structures, in the condition that the linear welding speed and all other variables are held constant.

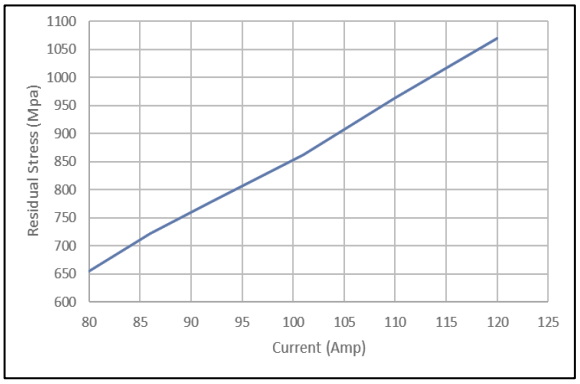

Fig 12 The Effect of the Amperage Changes on the Residual Stress.

5. Conclusions

1. Comparing the results of numerical simulation with practical measurement, the acceptable accuracy of simulations is presented with deviation between numerical solution and the practical method.
2. The magnitude of residual stress in the welding process excessed the yield stress.
3. The maximum residual stress occurred in the region near the fusion zone increase with a decreasing specimen thickness.
4. The surface between fusion zone and heat affected zone is susceptible of cracks resulted from welding residual stress.
5. When the weld heat input is increased residual stress level increase and vice versa.
6. The differences between measured and calculated residual stress results can be related to the following predominant factors: theoretical basis, temperature distribution, original residual stress strain gauge placement, mechanical grinding and the oxidation layer.

6. Acknowledgments

This work was supported by the Metal Laboratory of the Material Engineering Department, Basrah University. The authors also wish to express their great appreciation to Mr. M. R. Khnuba for their kind help in implementation of this program software (ANSYS) and to Mr. A. A. Hamdan for his effort in preparation of the experiment.

References

[1] Cleiton Carvalho Silva, Joaquim Teixeira de Assis, Sergey Philippov, and Jesualdo Pereira Farias, "Residual Stress, Microstructure and Hardness of Thin-Walled Low-Carbon Steel Pipes Welded Manually", Materials Research, Vol. 19, No. 6, 2016.

[2] Nurul Syahida Mohd Nasir, Mohammad Khairul Azhar Abdul Razab, Sarizam Mamat, Muhammad Iqbal Ahmad, "Review on Welding Residual Stress" ARPN Journal of Engineering and Applied Sciences, Vol. 11, No. 9, pp. 6166-6175, 2016.

[3] ASTM, "Standard Specification for Seamless Carbon Steel Pipe for High-Temperature Service", ASTM International, ASTM A106, 2016.

[4] ASTM, "Standard Test Method for Determining Residual Stresses by the Hole-Drilling Strain-Gage Method" ASTM International, ASTM E837, 2001.

[5] J. P. Hollman, Heat Transfer, Vol. I, John Wiley, 1985.

[6] E. R. Dhas, and S. Kumanan, "Weld Residual Stress Prediction Using Artificial Neural Network and Fuzzy Logic modeling", Indian Journal of Engineering and Materials Sciences, Vol. 18, pp. 351-360, 2011.

[7] ASME, "Standard for Welding and Brazing Procedures, Welders, Braziers, and Welding and Brazing Operators", ASME Section IX, ASME International, 2004.

[8] Hung-JuYen, Mark Ching-Cheng Lin, Lih-Jin Chen, "Measurement and Simulation of Residual Stress in Type 304 Weld Overlay Stainless Steel Pipe", Elsevier, International Journal of Pressure Vessels and Piping, Vol. 60, Issue 3, pp. 271-283, 1994.

[9] Tso-Liang Teng, Chih-Cheng Lin, "Effect of Welding Conditions on Residual Stresses due to Butt Welds", Elsevier, International Journal of Pressure Vessels and Piping, Vol. 75, Issue 12, pp. 857-864, 1998.

[10] Dieter Radaj, "Heat Effects of Welding", 1st Edition, Springer-Verlag Berlin Heidelberg, ISBN 978-3-642-48642-5 1992.

[11] Botjan Taljat, T. Zacharia, X. L. Wang, J. R. Keiser, R. W. Swindeman, Z. Feng, and M. J. Jirinec, "Numerical Analysis of Residual Stress Distribution in Tubes with Spiral Weld Cladding", Welding Journal-New York, Vol. 77, pp. 328-335, 1998.

[12] D. J. Smith, P. J. Bouchard, and D. George, "Measurement and Prediction of Residual Stresses in Thick-Section Steel Welds", Journal of Strain Analysis for Engineering Design, Vol. 35, No. 4, pp. 287-305, 2000.